Check for updates

NANO · MICRO small
www.small-journal.com

A Strong Acid-Induced DNA Hydrogel Based on pH-Reconfigurable A-Motif Duplex

*Yuwei Hu and Jackie Y. Ying**

Under a pH value lower than the pK_a of adenine (3.5), adenine-rich sequences (A-strand) form a unique parallel A-motif duplex due to the protonation of A-strand. At a pH above 3.5, deprotonation of adenines leads to the dissolution of A-motif duplex to A-strand single coil. This pH-reconfigurable A-motif duplex has been developed as a novel pH-responsive DNA hydrogel, termed A-hydrogel. The hydrogel state is achieved at pH 1.2 by the A-motif duplex bridging units, which are cross-linked by both reverse Hoogsteen interaction and electrostatic attraction. Hydrogel-to-solution transition is triggered by pH 4.3 due to the deprotonation-induced separation of A-motif duplex. The A-hydrogel system undergoes reversible hydrogel–solution transitions by subjecting the system to cyclic pH shifts between 1.2 and 4.3. An anti-inflammatory medicine, sulfasalazine (SSZ), which intercalates into A-motif duplex, is loaded into A-hydrogel. Its pH-controlled release from A-hydrogel is successfully demonstrated. The strong acid-induced A-hydrogel may fill the gap that other mild acid-responsive DNA hydrogels cannot do, such as protection of orally delivered drug in hostile stomach environment against strong acid (pH ~ 1.2) and digestive enzymes.

1. Introduction

Hydrogels, composed of three-dimensional (3D)-cross-linked polymer networks saturated with water, have been finely tuned[1,2] and used in a vast range of applications, including energy,[3] drug release,[4,5] water sustainability,[6,7] tissue engineering,[8] sensing,[9] cell culture,[10] soft robotics,[11] actuators,[12] ionotronics,[13] microelectronics,[14] etc. By adjusting the physicochemical properties of polymers, such as incorporation of stimuli-responsive elements, target recognition sites, and other functional materials, multi-functional hydrogels could be achieved to meet the demands for advanced applications.

Y. Hu, J. Y. Ying
NanoBio Lab
Institute of Materials Research and Engineering
Agency for Science, Technology and Research (A*STAR)
31 Biopolis Way, The Nanos, #09-01, Singapore 138669, Singapore
E-mail: jyying@imre.a-star.edu.sg
J. Y. Ying
NanoBio Lab
A*STAR Infectious Diseases Labs
A*STAR
31 Biopolis Way, The Nanos, #09-01, Singapore 138669, Singapore
The ORCID identification number(s) for the author(s) of this article can be found under https://doi.org/10.1002/smll.202205909.

DOI: 10.1002/smll.202205909

Beyond its critical genetic encoding roles in RNA transcription and protein translation, DNA as a polymer consisting of nucleotides has been extensively studied and applied in various fields.[15–18] Recently, DNA hydrogels, which use hybridized DNA duplex strands as the cross-linking scaffolds, have attracted a great deal of research interest.[19–22] To generate 3D networks, entanglements of either DNA strands or DNA-polymer composites have been developed. Besides Watson–Crick hybridization interaction cross-linked duplex,[23–25] various other structures, such as pH-driven formation of $C^+ \cdot G–C$ and $T \cdot A–T$ triplex,[26,27] pH-stimulated assembly of cytosine-rich strands into i-motif configurations,[28] K^+-triggered assembly of guanine-rich strands into G-quadruplex,[29] metal ion co-bridged duplexes ($C–Ag^+–C$ or $T–Hg^{2+}–T$),[30,31] light-activated *trans*/*cis*-azobenzene units or *o*-nitrobenzylphosphate ester modified oligonucleotides,[32,33] ligand–aptamer complexes,[34] DNAzymes,[35] enzymes,[36] and CRISPR systems,[37] have been incorporated into smart DNA hydrogels. Hence, external stimuli, e.g., pH, metal ions, light, temperature, oligonucleotides, small molecules, and chemical reactions, have been used to induce DNA hydrogel's physicochemical property changes involving shape, stiffness, size, fluorescence, hydrogel-to-liquid or hydrogel-to-solid transitions.[20] Furthermore, these stimuli-triggered processes could be reversed in the presence of respective counter triggers.

Among these stimuli-responsive DNA hydrogels, pH-triggered assembly and disassembly of the system may find interesting applications in mildly acidic tumor microenvironment or compartments of cells (e.g., endosomes and lysosomes) for biological information processing, as well as targeted drug delivery and therapy.[38,39] Currently reported pH-responsive DNA hydrogels mainly use triplex ($C^+ \cdot G–C$ and $T \cdot A–T$)[40–44] and i-motif configurations[45–50] as the pH-sensing elements, which respond to the mildly acidic pH range of 5.0–7.0. Taking i-motif-based DNA hydrogels for example, the hydrogel state would form at pH 5.0 cross-linked by i-motif structures, and the solution state would occur at pH 7.0 due to the dissolution of i-motif linking units. DNA hydrogels responding to a pH range of 1.0–4.0 are rarely reported due to the instability of DNA strands. For example, depurination of oligodeoxynucleotides happens at low pH values, resulting in apurinic sites, whereby covalent structures of DNA are more susceptible to damage. However,

 © 2023 Wiley-VCH GmbH

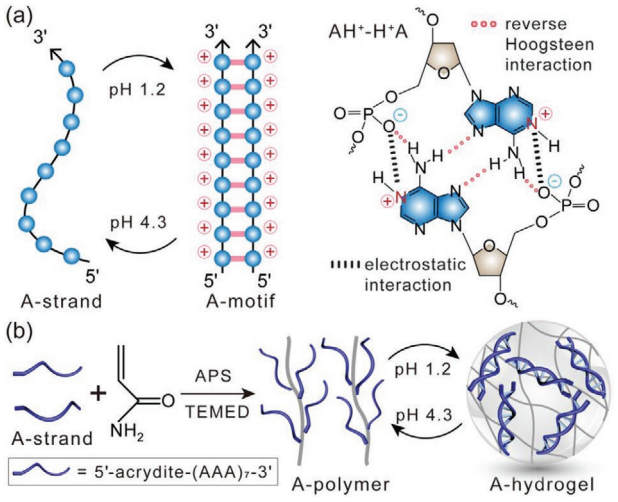

Figure 1. Schematic demonstration of a) pH-switchable transformation between A-strand single coil and parallel A-motif duplex, as well as the chemical structure of protonated AH^+-H^+A pairing, and b) chemical synthesis of A-strand-polyacrylamide copolymers (A-polymers) and reversible pH-triggered solution/hydrogel transitions.

depurination depends greatly on the DNA sequences. Studies showed that the order of depurination rates of DNA sequences at low pH values was $(AT)_{15} \geq (N)_{30} > (AG)_{15} > (AC)_{15} > (A)_{30}$, with an extremely slow rate for $(A)_{30}$ (N = A, T, G, or C).[51]

In this study, by using A-motif as the pH-reconfigurable element, we introduced a novel strong acid-induced DNA hydrogel, termed A-hydrogel. A-hydrogel remained in the hydrogel state cross-linked by A-motif parallel duplex at a pH range of 1.2–3.2, and dissociated into solution at pH 4.3 due to the disassembly of A-motif into A-strand single coil (**Figure 1**). The phase transitions between strong acid-induced hydrogel state and mild-acid dissociated solution state were reversible by subjecting the system to cyclic pH shifts between 1.2 and 4.3. As a proof of concept for controlled drug release, sulfasalazine (SSZ), an anti-inflammatory medication to treat ulcerative colitis, Crohn's disease and other types of inflammatory bowel disease, was encapsulated into A-hydrogel, and its pH-triggered release from A-hydrogel was demonstrated.

2. Results and Discussion

Adenine-rich sequence (A-strand) is a tail component of mRNA in all eukaryotic cells, and it plays a key role in the stability of mRNA and translation initiation. Under neutral or alkaline pH, A-strand would exist as right-handed, single-stranded conformation stabilized by π–π stacking of adenines, while at acidic pH values (<3.5), the protonation of adenines (pK_a = 3.5) would lead to the structural reconfiguration to parallel A-motif duplex.[52,53] In this conformation, A-motif could be stabilized by AH^+–H^+A units, in which hydrogen bonds (reverse Hoogsteen interaction) would be formed between protonated adenines, along with electrostatic attraction between the positively charged protons at the N(1) position of adenines and the negatively charged phosphate groups (Figure 1a).[54] The pH-responsive structural transitions were reversible.

Based on the pH-triggered configuration transitions of A-strand, 5′-acrydite modified A-strands were copolymerized with acrylamide monomers by free radical polymerization to form A-strand-polyacrylamide copolymers (A-polymers), which formed hydrogel state at pH 1.2 by the cross-linking of A-motif duplex. The hydrogel dissociation into solution state happened at pH 4.3 (Figure 1b). No hydrogel formation was observed by either polyacrylamide alone or A-strands alone when the pH was changed to 1.2. Thus, a strong acid-induced DNA hydrogel was prepared by using A-motif as the pH-sensing elements and polyacrylamide as the backbones. In A-polymer, the ratio of DNA subunits to unsubstituted acrylamide units was determined spectroscopically to be 1:19 (for the determination of the loading, see Figure S1, Supporting Information).

Low pH-induced A-motif formation was recently reported to facilitate the binding of thiol DNA to gold nanoparticles (Au NPs),[55] generate DNA architectures,[56] and colorimetric DNA sensor.[57] In addition, A-strand showed high binding affinity to Au NPs, which was developed to program NP valence bonds.[58] Studies revealed that A-strand exhibited excellent stability in the pH range of 1.0–7.0 as compared to guanine-rich strand, which had much shorter half-life than A-strand.[55] It was also found that depurination, the release of purine bases from nucleic acids by the hydrolysis of *N*-glycosidic bonds, was extremely low for A-strand at low pH values in contrast to random sequences, guanine-rich strands, or adenine-thymine strands.[51] In this study, thermal melting behavior of A-strand in pH 1.2 PBS buffer was studied with UV–vis spectroscopy, which showed a well-defined sigmoidal thermal transition, **Figure 2**a, demonstrating the dissolution of cooperatively held A-motif duplex to A-strand single coil. However, the thermally induced transitions might not be considered as fully reversible since adenosine homopolymers undergo depurination at elevated temperatures,[53] as evidenced by the gel electrophoresis (Figure 2a inset). When heated to 95 °C under pH 1.2, a faint A-strand band was observed as compared to that at room temperature, indicating the instability of A-strand under these conditions. The A-strand bands at pH 4.3 and 8.0 showed no obvious difference in intensity, indicating that A-strand possessed similar thermal stability. The slight curvature of bands on the right might be caused by the applied high voltage (240 V) in running PAGE. From the UV–vis thermal melting profile, the T_m of A-strand under pH 1.2 PBS buffer corresponded to ~ 80 °C, which was consistent with previous study.[53] A broad and non-cooperative melting profile was obtained at pH 4.3 (Figure S2, Supporting Information), demonstrating that A-strand single coil was stabilized largely by π–π stacking interactions at pH above 3.5.[53]

Circular dichroism (CD) was used to verify the formation of A-motif and its dissociation into A-strand under different pH values. At pH 1.2, an intense, positive band that peaked at 264 nm with a shoulder at 272 nm and negative bands centered at 243 and 209 nm were observed, which indicated the parallel A-motif duplex structures (Figure 2b).[53] At pH 4.3, A-polymer showed a strong positive band that peaked at 217 nm with a shoulder at 230 nm, a weak positive band at 275 nm, and negative bands centered at 250 and 207 nm, which were characteristics of single-stranded A-strand.[53]

© 2023 Wiley-VCH GmbH

16136829, 2023, 12, Downloaded from https://onlinelibrary.wiley.com/doi/10.1002/smll.202205909 by Guangzhou University, Wiley Online Library on [20/02/2024]. See the Terms and Conditions (https://onlinelibrary.wiley.com/terms-and-conditions) on Wiley Online Library for rules of use; OA articles are governed by the applicable Creative Commons License

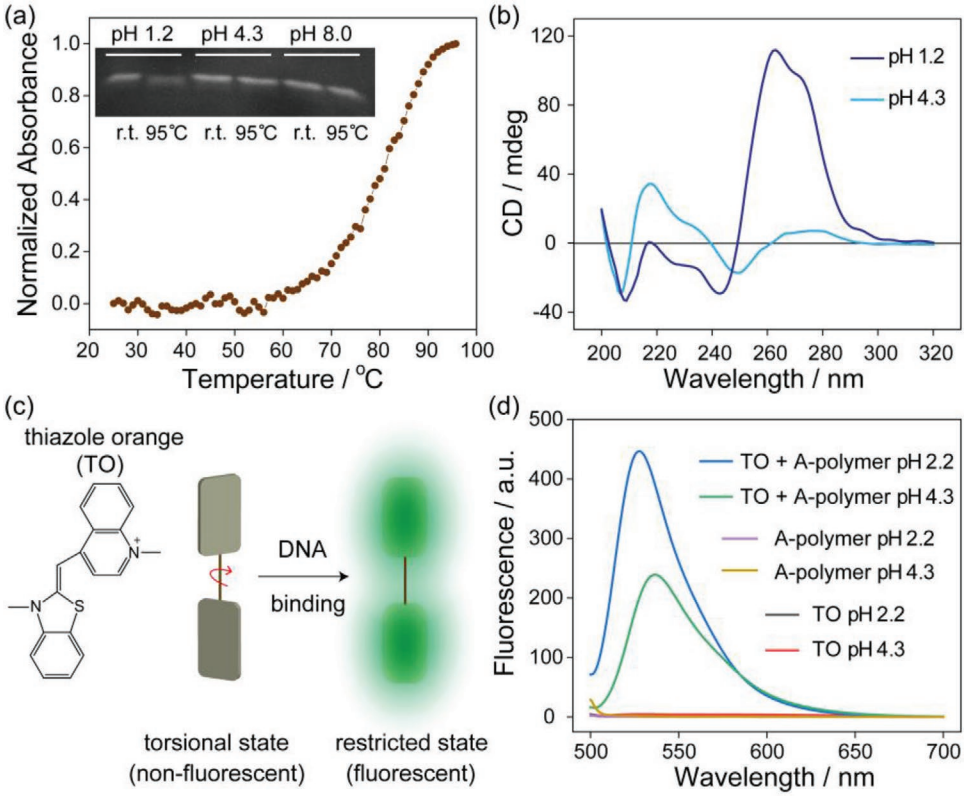

Figure 2. a) Thermal melting profile of A-strand at pH 1.2 PBS buffer recorded by UV–vis spectroscopy. Inset showed the denaturing PAGE of A-strand under pH 1.2, 4.3, and 8.0 at room temperature (r.t.) and 95 °C. b) CD spectra of A-polymer recorded in PBS buffer of pH 1.2 and 4.3. c) Chemical structure of TO, and a schematic representation of its internal torsional movement (aromatic subunits are depicted by rotating plates) and restricted motion (high fluorescence state) upon binding to duplex DNA. d) Fluorescence spectra of A-polymer, TO, as well as TO with A-polymer under pH 2.2 and 4.3 in PBS buffer.

To further confirm the A-motif duplex and A-strand single coil configurations, an asymmetrical cyanine, thiazole orange (TO), consisting of conjugated benzothiazole and quinoline aromatic rings connected by one bridging methine bond, was employed as the fluorescence indicator (Figure 2c).[59] Due to the low molar ratio of TO cation at pH 1.2,[60] its fluorescence was recorded at pH 2.2 and compared to that at pH 4.3. When TO was free in solution, negligible fluorescence was obtained at either pH 2.2 or 4.3 due to intramolecular twisting motions around the methine bond, which resulted in a rapid non-radiative decay of the excited state (Figure 2d). At pH 4.3, A-strand in -polymer (consisting of polyacrylamide backbones and A-strand tethers) existed as single coil, and a low magnitude of TO fluorescence signal was observed. Upon pH 2.2 triggered transition from A-strand single coil to A-motif duplex, TO intercalated or stacked between base pairs and inside grooves of the duplex in A-polymer, leading to constricted torsional motion within the dye and planarity between the twisting segments, which resulted in a markedly increased fluorescence. These results were consistent with previous studies, which demonstrated that TO bound to duplex DNA with high affinity and to single-stranded polypurines with lower affinity, corresponding to high and low fluorescence signal, respectively.[60] It was noteworthy that no fluorescence was observed in A-polymer at either pH 2.2 or 4.3 (Figure 2d), eliminating the fluorescence contribution from polyacrylamide. Similar results were observed for the mixture of TO and A-motif (not A-polymer) at pH 2.2 and 4.3 (Figure S3, Supporting Information). To the best of our knowledge, this is the first demonstration of using TO to probe A-motif duplex formation. However, more experimental and theoretical studies are needed to fully understand their interactions and mechanisms, as well as the differentiation to B-DNA duplex.

After verifying the pH-triggered A-motif duplex formation, disassembly and thermal stability, A-motif cross-linked DNA hydrogel (A-hydrogel) was achieved. Complementary rheometry characterizations were performed to provide physical insight into the pH-reconfigurable A-hydrogel (**Figure 3**). Figure 3a depicts the rheometric features of A-hydrogel. At pH 1.2, A-hydrogel revealed a storage modulus of G' = 38 Pa, and a loss modulus of G'' = 2 Pa. These values were consistent with the formation of a hydrogel (G'/G'' = 19). When the pH value was adjusted to 4.3, the A-hydrogel transitioned to a liquid phase ($G' \sim G'' \sim$ 1–3 Pa) due to the dissociation of A-motif cross-linking units to A-strand single coils. Figure 3b depicts the switchable G' and G'' values transitioned between hydrogel and liquid states upon cyclic pH triggers. A decrease in G' value was observed upon the second pH switching cycle. During rheological measurements, the probe of rheometer would come in contact with the hydrogel. Under an applied force, the hydrogel would be distorted during the measurements, which would lead to its physical damage. The

© 2023 Wiley-VCH GmbH

16136829, 2023, 12, Downloaded from https://onlinelibrary.wiley.com/doi/10.1002/smll.202205909 by Guangzhou University, Wiley Online Library on [20/02/2024]. See the Terms and Conditions (https://onlinelibrary.wiley.com/terms-and-conditions) on Wiley Online Library for rules of use; OA articles are governed by the applicable Creative Commons License

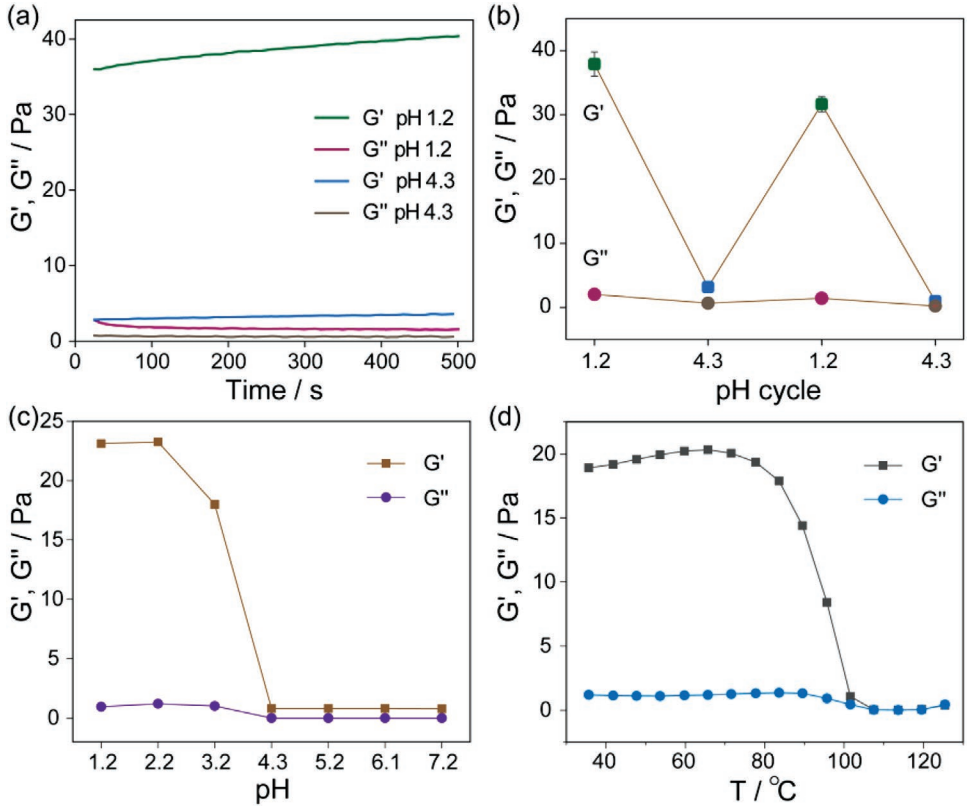

Figure 3. a) Rheological studies of A-hydrogel under pH 1.2 and 4.3. b) Rheological measurements of switchable hydrogel-solution states by using pH as triggers. c) Rheological measurements of pH-induced transformation of A-hydrogel into liquid state. d) Rheological measurements of temperature-induced transition of A-hydrogel into liquid state.

pH-dependent hydrogel-liquid transitions are demonstrated in Figure 3c, showing a hydrogel state under strong acids (pH 1.2, 2.2, and 3.2) and liquid state at pH > 4.3. The thermal stability of A-hydrogel was measured and presented as Figure 3d. Starting at ~80 °C, sharp decrease in the storage modulus (G') was observed with rheological measurements, indicating the transformation of the hydrogel into a liquid phase. To further verify the A-motif cross-linked A-hydrogel, thymine-rich strands (T-strands) were introduced into A-polymer to block A-strand by forming A–T duplexes based on Watson–Crick base-pairing interactions, which remained as a liquid state at pH 4.3. When the system pH was adjusted to 1.2, a hydrogel state was observed. The melting profile of A–T fully hybridized duplex showed a T_m value of ~60 °C at pH 4.3 (Figure S4, Supporting Information). The higher cooperative dissociation temperature of A-motif, centered at ~80 °C, as compared to that of A–T duplex (~60 °C) demonstrated a higher binding affinity of A-motif under pH 1.2, leading to the disassembly of A–T duplex and formation of A-motif, and therefore a hydrogel state.

Scanning electron microscopy (SEM) was also conducted to verify the hydrogel and solution states. **Figure 4**a shows the SEM image of A-hydrogel at pH 1.2. A porous cross-linked network was observed, consistent with the typical morphology of a hydrogel matrix. The images in Figure 4b depicted the cyclic pH-stimulated hydrogel state to liquid state transitions. At pH 1.2, a hydrogel state was observed, which changed to liquid state when the pH was adjusted to 4.3. The pH-triggered hydrogel-to-liquid transitions were reversible. The stability of A-hydrogel was also examined in pH 1.2 and 4.3 buffers, as depicted in Figure 4c. To facilitate studies on the hydrogel, the latter was stained with GelRed. When transferred into pH 1.2 buffer, A-hydrogel remained in the hydrogel state as demonstrated by the red piece at the bottom of the tube. When placed in pH 4.3 buffer, A-hydrogel dissociated into solution and the red-colored gel disappeared. pH-indicator papers were inserted into the tubes to show the pH values of the buffers.

SSZ is a well-known commercial prodrug to treat irritable bowel syndrome, Crohn's disease, and ulcerative colitis.[61] The planar rings of SSZ moiety could partially intercalate into DNA duplex structures base-paired by Watson–Crick interactions.[62] Though A-motif duplex was stabilized by AH^+–H^+A units via reverse Hoogsteen interaction and electrostatic interaction and adopted a 12° tilt from the horizontal to the helical axis,[53] the formed planar adenine base pairs still provided the anchoring point for SSZ binding via intercalation and stacking, which was also evident in the studies of TO binding to A-motif. Before loading SSZ into A-hydrogel for pH-controlled release, its pH-dependent absorbance behavior was first studied with an identical concentration under various pH values (Figure S5, Supporting Information). The maximum absorbance red-shifted slightly from 353, 354, 358 to 360 nm with the increase of pH values from pH 1.2, 2.2, 3.2, to 4.3, respectively. A maximum absorbance intensity difference of 7% between pH 1.2 and 4.3 was observed. These red shifts and intensity changes were not significant, and the absorbance of SSZ could

© 2023 Wiley-VCH GmbH

16136829, 2023, 12, Downloaded from https://onlinelibrary.wiley.com/doi/10.1002/smll.202205909 by Guangzhou University, Wiley Online Library on [20/02/2024]. See the Terms and Conditions (https://onlinelibrary.wiley.com/terms-and-conditions) on Wiley Online Library for rules of use; OA articles are governed by the applicable Creative Commons License

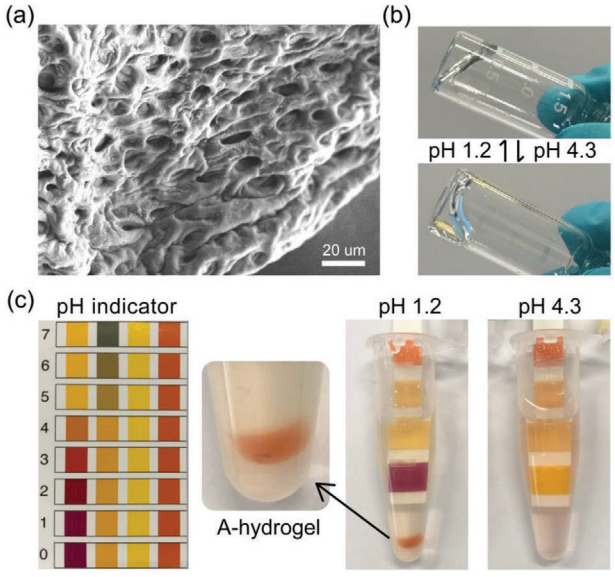

Figure 4. a) SEM image illustrating the 3D cross-linked networks in A-hydrogel. b) Photographs showing the pH-switchable hydrogel state and solution state at pH 1.2 and 4.3, respectively. c) Photographs showing that the A-hydrogel remained in the hydrogel state when immersed in pH 1.2 buffer, and dissociated into solution in pH 4.3 buffer. pH-indicator papers indicated the pH values of the buffer. A-hydrogel was stained with GelRed for better illustration.

be considered as pH-independent. Therefore, SSZ was loaded into the A-motif duplex cross-linked A-hydrogel, and its release upon pH-triggered dissolution of the hydrogel was examined. Details on loading of SSZ into A-hydrogel and its release processes could be found in the experimental section. At pH 1.2 and 2.2, minimum SSZ was released from A-hydrogel (see Figure S6, Supporting Information, for the corresponding UV–vis spectra of released SSZ in solutions). Based on the absorbance-concentration calibration curve of SSZ at different pH values (Figure S7, Supporting Information), only 4% of loaded SSZ was released at a time interval of 60 min under pH 1.2 and 2.2. At pH 3.2, a slightly increased amount of SSZ, 14%, was obtained from A-hydrogel after the same time interval (**Figure 5**a). The increased release of SSZ might be attributed to the slight instability of A-motif at pH 3.2, which was approaching the pK_a value (3.5) of adenines. At pH 4.3, rapid SSZ release from A-hydrogel was obtained (Figure 5b). After a time interval of 60 min, 97% of the loaded SSZ was released, which was accompanied by the complete dissolution of A-hydrogel. Figure 5c depicts the normalized time-dependent release profiles of SSZ upon treatment of the SSZ-loaded A-hydrogel under conditions of pH 1.2, 2.2, 3.2, and 4.3. Sequential release profile of the loaded SSZ from A-hydrogel at pH 1.2 and 4.3 was also examined and plotted in Figure 5d. In general, 4% and 92% of the loaded SSZ were released under pH 1.2 and 4.3 from A-hydrogel, respectively. The UV–vis spectra of SSZ released at pH 4.3 are presented as Figure S8 (Supporting Information).

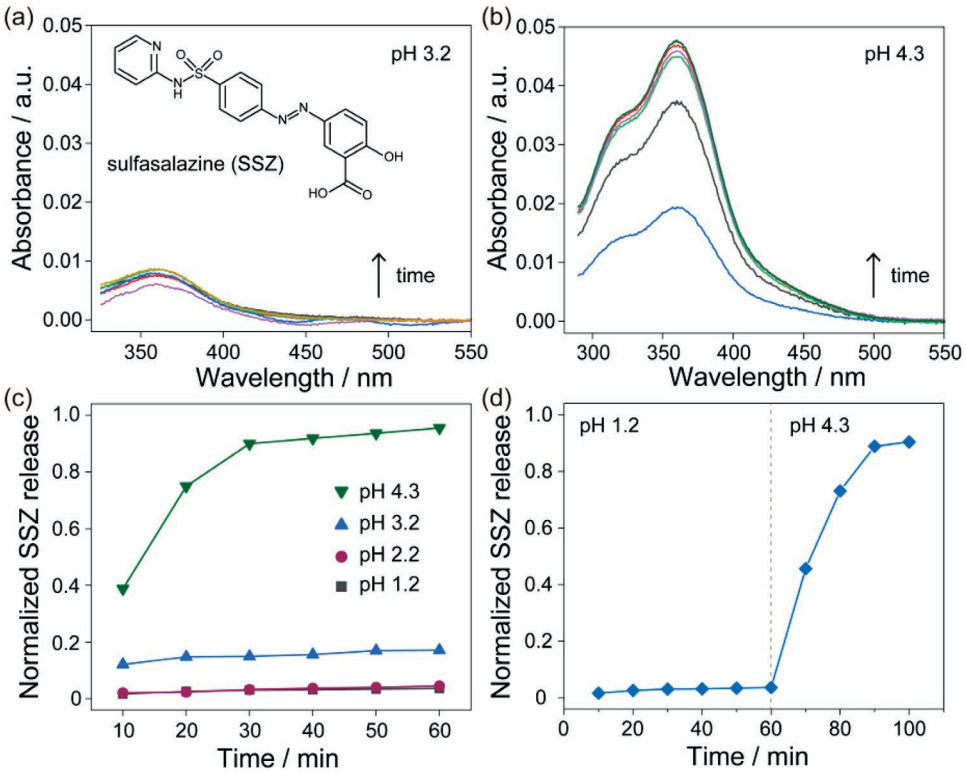

Figure 5. UV–vis spectra of SSZ released from A-hydrogel at a) pH 3.2 and b) 4.3. Inset in (a) is the chemical structure of SSZ. c) Normalized time-dependent release profiles of SSZ from A-hydrogel at pH 1.2, 2.2, 3.2, and 4.3. d) Normalized sequential release profile of SSZ from A-hydrogel under pH 1.2 and 4.3.

© 2023 Wiley-VCH GmbH

16136829, 2023, 12, Downloaded from https://onlinelibrary.wiley.com/doi/10.1002/smll.202205909 by Guangzhou University, Wiley Online Library on [20/02/2024]. See the Terms and Conditions (https://onlinelibrary.wiley.com/terms-and-conditions) on Wiley Online Library for rules of use; OA articles are governed by the applicable Creative Commons License

3. Conclusion

In conclusion, we have designed a novel DNA hydrogel, termed A-hydrogel, cross-linked by pH-reconfigurable A-motif parallel duplex. At a pH value lower than the pK_a (3.5) of adenines, protonation of A-strand led to the formation of parallel A-motif duplex, which served as the cross-linking units to generate a 3D network for a DNA hydrogel. When the system pH was adjusted to above the pK_a value, e.g., 4.3, deprotonation of adenines resulted in the disassembly of A-motif duplex to A-strand single coil, which led to the dissolution of A-hydrogel to a solution state. The phase transitions between strong acid-induced hydrogel and mild acid-dissociated solution were reversible by using pH triggers. Moreover, a sample drug, SSZ, was loaded into A-hydrogel by intercalation into the DNA duplex conformation, and its controlled pH-responsive release was demonstrated. Unlike most other pH-responsive DNA hydrogels that were triggered by mild acid, e.g., pH 5.0, our A-motif cross-linked DNA hydrogel would work in oral drug delivery and soft robotics in a strongly acidic environment. For instance, drugs loaded in A-hydrogel would be protected from the hostile environment in stomach. The A-hydrogel would remain in the hydrogel state under a strongly acidic condition (pH 1.2), and shield the drugs from digestive enzymes. It would provide controlled drug release in mild acid or neutral pH environments, including duodenum, small intestine, or colon.

Another well-studied pH-responsive DNA configuration, i-motif quadruplex, consisting of cytosine rich sequences, is triggered by mild acid, e.g., pH 5.0, and separates under neutral pH. Its structures and pH-responsiveness are completely different to A-motif, which is a parallel duplex and forms under highly acidic conditions, e.g., pH 1.2, and disassembles under mildly acidic pH. A comprehensive comparison between these two configurations as well as pH-triggered triplexes in structures, pH-responsiveness and their construction in DNA hydrogels is illustrated in our review article.[63]

4. Experimental Section

Materials: Magnesium chloride, ammonium persulfate (APS), *N,N,N′,N′*-tetramethylethylenediamine (TEMED), acrylamide solution (40%), pH-indicator paper, TO, SSZ and other chemicals were purchased from Sigma–Aldrich, unless otherwise noted. Desalted 5′ end acrydite-modified nucleic acid strand was purchased from Integrated DNA Technologies Inc. (Coralville, IA). The 15% Criterion TBE-Urea Polyacrylamide Gel was purchased from Bio-Rad. Ultrapure water purified by a Milli-Q system was used to prepare the solutions. The sequences used in the study are:

A-strand: 5′5″-acry-AAA AAA AAA AAA AAA AAA AAA-3′3″

T-strand: 5′5″-TTT TTT TTT TTT TTT TTT TTT-3′3″

Synthesis of the Acrylamide/Acrydite-Nucleic Acid Copolymers (A-Polymer): A 400-µL buffer solution (PBS, 10 mM, $MgCl_2$, 10 mM, pH 7.2) that included 2% acrylamide and the adenine-rich strand (0.6 mM) was prepared. Nitrogen was bubbled through the solution. Twenty-eight microliters of a 0.2-mL aqueous solution that included APS (20 mg) and TEMED (10 µL) was added to the mixture. The resulting solution was allowed to polymerize at room temperature for 5 min, and then the solution was further polymerized at 4 °C for 12 h. The resulting copolymer was purified from unreacted monomer units, salts, and initiators, using an Amicon (Millipore) spin filter unit (MWCO 10 kDa). The purified copolymer was removed from the filter and dried under a gentle nitrogen flow. The dried copolymer was redispersed into PBS buffer for further experiments, unless otherwise noted. The concentrations of the copolymer and the ratio of the acrylamide/acrydite-nucleic acid units were determined spectroscopically.

Fluorescence of TO: The fluorescence of TO (37.5 µM) was measured in pH 2.2 or 4.3 PBS buffer (10 mM, $MgCl_2$, 10 mM) in the presence or absence of A-polymer (3 µM). The measurements were conducted by fluorescence spectrophotometer (Hitachi, Model F-7100, Japan). The excitation wavelength was 482 nm, and the spectrum was recorded for 500–700 nm.

UV–Vis Spectra: UV–vis spectra were collected with Cary 3500 Compact Peltier UV–vis Spectrophotometer (Agilent) equipped with a thermal controller component. The melting curve was recorded with the absorbance at a wavelength of 260 nm.

Gel Electrophoresis: Denaturing polyacrylamide gel electrophoresis (PAGE) was conducted to confirm the thermal stability of A-strand under pH 1.2, 4.3, and 8.0 upon heating to 95 °C. The pH values of all samples were adjusted to neutral before running PAGE at 240 V.

SEM Imaging: SEM image was obtained with a field emission scanning electron microscope (JEOL JSM-7400F, Japan).

CD Spectra: The CD spectra of A-polymer under pH 1.2 and 4.3 were recorded in PBS buffer with JASCO J-815 CD Spectrometer.

Rheology Measurements: The mechanical properties of A-hydrogel were characterized by HAAKE MARS Rheometer (Thermo Scientific). The samples were placed onto parallel-plate geometry (35 mm in diameter) at a temperature of 25 °C. The linear viscoelastic region was found to be in the range of 1% strain and 1 Hz frequency.

Loading of SSZ into A-Hydrogel and pH-Triggered Release of SSZ: One microliter SSZ (0.1 M, DMSO) was added into 10 µL of A-polymer at neutral pH. One microliter HCl (1.5%) was used to change the mixture to hydrogel state. This was followed by adding 200 µL of pH 1.2 PBS buffer. To examine the SSZ release from A-hydrogel, 1 µL of solution was taken in 10 min intervals, and added into 200 µL of pH 1.2 PBS buffer. The absorbance of SSZ was recorded by UV–vis spectrophotometer. The same procedure was adopted for the release measurements in pH 2.2, 3.2, and 4.3 PBS buffers. For the sequential release of SSZ under pH 1.2 and 4.3, 1.5 µL of NaOH (18 M) was added into pH 1.2 PBS buffer (200 µL) to change the pH to 4.3. The completely released concentration of SSZ was 2.5 µM based on the added amount. The released amount of SSZ under various pH values was calculated using the absorbance-concentration calibration curve, and the release percentage was obtained by comparing the amount to 2.5 µM.

Supporting Information

Supporting Information is available from the Wiley Online Library or from the author.

Acknowledgements

This work was supported by the Health and Biomedical Sciences Industry Alignment Fund Pre-Positioning (IAF-PP) (grant no. H20H7a0034), Singapore. Y.H. acknowledges the support by Career Development Fund (CDF) (C210112014), and SERC Central Research Fund (CRF, UIBR, KIMR220901aSERCRF), A*STAR, Singapore.

Conflict of Interest

The authors declare no conflict of interest.

Data Availability Statement

The data that support the findings of this study are available from the corresponding author upon reasonable request.

© 2023 Wiley-VCH GmbH

16136829, 2023, 12, Downloaded from https://onlinelibrary.wiley.com/doi/10.1002/smll.202205909 by Guangzhou University, Wiley Online Library on [20/02/2024]. See the Terms and Conditions (https://onlinelibrary.wiley.com/terms-and-conditions) on Wiley Online Library for rules of use; OA articles are governed by the applicable Creative Commons License

Keywords

adenine, A-motif, DNA hydrogel, duplex, strong acid

Received: September 26, 2022
Revised: December 7, 2022
Published online: January 1, 2023

[1] J. Y. Sun, X. Zhao, W. R. Illeperuma, O. Chaudhuri, K. H. Oh, D. J. Mooney, J. J. Vlassak, Z. Suo, *Nature* **2012**, *489*, 133.
[2] Q. Wang, J. L. Mynar, M. Yoshida, E. Lee, M. Lee, K. Okuro, K. Kinbara, T. Aida, *Nature* **2010**, *463*, 339.
[3] Y. Guo, J. Bae, Z. Fang, P. Li, F. Zhao, G. Yu, *Chem. Rev.* **2020**, *120*, 7642.
[4] N. A. Peppas, J. Z. Hilt, A. Khademhosseini, R. Langer, *Adv. Mater.* **2006**, *18*, 1345.
[5] C. Ma, Y. Shi, D. A. Pena, L. Peng, G. Yu, *Angew. Chem., Int. Ed.* **2015**, *54*, 7376.
[6] X. Zhou, Y. Guo, F. Zhao, G. Yu, *Acc. Chem. Res.* **2019**, *52*, 3244.
[7] Y. Guo, L. S. de Vasconcelos, N. Manohar, J. Geng, K. P. Johnston, G. Yu, *Angew. Chem., Int. Ed.* **2022**, *61*, e202114074.
[8] S. Jiang, Z. Cao, *Adv. Mater.* **2010**, *22*, 920.
[9] D. Buenger, F. Topuz, J. Groll, *Prog. Polym. Sci.* **2012**, *37*, 1678.
[10] M. W. Tibbitt, K. S. Anseth, *Biotechnol. Bioeng.* **2009**, *103*, 655.
[11] Y. Lee, W. J. Song, J. Y. Sun, *Mater. Today Phys.* **2020**, *15*, 100258.
[12] X. Le, W. Lu, J. Zhang, T. Chen, *Adv. Sci.* **2019**, *6*, 1801584.
[13] C. Yang, Z. Suo, *Nat. Rev. Mater.* **2018**, *3*, 125.
[14] Y. Liu, J. Liu, S. Chen, T. Lei, Y. Kim, S. Niu, H. Wang, X. Wang, A. M. Foudeh, J. B. Tok, Z. Bao, *Nat. Biomed. Eng.* **2019**, *3*, 58.
[15] N. C. Seeman, H. F. Sleiman, *Nat. Rev. Mater.* **2017**, *3*, 17068.
[16] O. I. Wilner, I. Willner, *Chem. Rev.* **2012**, *112*, 2528.
[17] F. Wang, C. H. Lu, I. Willner, *Chem. Rev.* **2014**, *114*, 2881.
[18] E. Del Grosso, E. Franco, L. J. Prins, F. Ricci, *Nat. Chem.* **2022**, *14*, 600.
[19] F. Li, J. Tang, J. Geng, D. Luo, D. Yang, *Prog. Polym. Sci.* **2019**, *98*, 101163.
[20] J. S. Kahn, Y. Hu, I. Willner, *Acc. Chem. Res.* **2017**, *50*, 680.
[21] J. Li, L. Mo, C. H. Lu, T. Fu, H. H. Yang, W. Tan, *Chem. Soc. Rev.* **2016**, *45*, 1410.
[22] D. Wang, Y. Hu, P. Liu, D. Luo, *Acc. Chem. Res.* **2017**, *50*, 733.
[23] A. Cangialosi, C. Yoon, J. Liu, Q. Huang, J. Guo, T. D. Nguyen, D. H. Gracias, R. Schulman, *Science* **2017**, *357*, 1126.
[24] S. H. Um, J. B. Lee, N. Park, S. Y. Kwon, C. C. Umbach, D. Luo, *Nat. Mater.* **2006**, *5*, 797.
[25] J. B. Lee, S. Peng, D. Yang, Y. H. Roh, H. Funabashi, N. Park, E. J. Rice, L. Chen, R. Long, M. Wu, D. Luo, *Nat. Nanotechnol.* **2012**, *7*, 816.
[26] Y. Hu, A. Cecconello, A. Idili, F. Ricci, I. Willner, *Angew. Chem., Int. Ed.* **2017**, *56*, 15210.
[27] A. Idili, A. Vallee-Belisle, F. Ricci, *J. Am. Chem. Soc.* **2014**, *136*, 5836.
[28] Y. Dong, Z. Yang, D. Liu, *Acc. Chem. Res.* **2014**, *47*, 1853.
[29] M. Di Antonio, A. Ponjavic, A. Radzevicius, R. T. Ranasinghe, M. Catalano, X. Zhang, J. Shen, L. M. Needham, S. F. Lee, D. Klenerman, S. Balasubramanian, *Nat. Chem.* **2020**, *12*, 832.
[30] W. Guo, X. J. Qi, R. Orbach, C. H. Lu, L. Freage, I. Mironi-Harpaz, D. Seliktar, H. H. Yang, I. Willner, *Chem. Commun.* **2014**, *50*, 4065.
[31] X. Xue, F. Wang, X. Liu, *J. Am. Chem. Soc.* **2008**, *130*, 3244.
[32] H. Kang, H. Liu, X. Zhang, J. Yan, Z. Zhu, L. Peng, H. Yang, Y. Kim, W. Tan, *Langmuir* **2011**, *27*, 399.
[33] F. Huang, M. Chen, Z. Zhou, R. Duan, F. Xia, I. Willner, *Nat. Commun.* **2021**, *12*, 2364.
[34] H. Yang, H. Liu, H. Kang, W. Tan, *J. Am. Chem. Soc.* **2008**, *130*, 6320.
[35] S. Lilienthal, Z. Shpilt, F. Wang, R. Orbach, I. Willner, *ACS Appl. Mater. Interfaces* **2015**, *7*, 8923.
[36] L. Heinen, T. Heuser, A. Steinschulte, A. Walther, *Nano Lett.* **2017**, *17*, 4989.
[37] M. A. English, L. R. Soenksen, R. V. Gayet, H. D. Puig, N. M. Angenent-Mari, A. S. Mao, P. Q. Nguyen, J. J. Collins, *Science* **2019**, *365*, 780.
[38] X. Guo, F. Li, C. Liu, Y. Zhu, N. Xiao, Z. Gu, D. Luo, J. Jiang, D. Yang, *Angew. Chem., Int. Ed.* **2020**, *59*, 20651.
[39] P. Peng, Y. Du, J. Zheng, H. Wang, T. Li, *Angew. Chem., Int. Ed.* **2019**, *58*, 1648.
[40] Y. Hu, W. Guo, J. S. Kahn, M. A. Aleman-Garcia, I. Willner, *Angew. Chem., Int. Ed.* **2016**, *55*, 4210.
[41] Y. Hu, A. Cecconello, A. Idili, F. Ricci, I. Willner, *Angew. Chem., Int. Ed.* **2017**, *56*, 15210.
[42] Y. Hu, C.-H. Lu, W. Guo, M. A. Aleman-Garcia, J. Ren, I. Willner, *Adv. Funct. Mater.* **2015**, *25*, 6867.
[43] J. Ren, Y. Hu, C. H. Lu, W. Guo, M. A. Aleman-Garcia, F. Ricci, I. Willner, *Chem. Sci.* **2015**, *6*, 4190.
[44] C. Wang, A. Fischer, A. Ehrlich, Y. Nahmias, I. Willner, *Chem. Sci.* **2020**, *11*, 4516.
[45] E. Cheng, Y. Xing, P. Chen, Y. Yang, Y. Sun, D. Zhou, L. Xu, Q. Fan, D. Liu, *Angew. Chem., Int. Ed.* **2009**, *48*, 7660.
[46] W. Guo, C. H. Lu, X. J. Qi, R. Orbach, M. Fadeev, H. H. Yang, I. Willner, *Angew. Chem., Int. Ed.* **2014**, *53*, 10134.
[47] Y. Hu, J. S. Kahn, W. Guo, F. Huang, M. Fadeev, D. Harries, I. Willner, *J. Am. Chem. Soc.* **2016**, *138*, 16112.
[48] Y. Shao, H. Jia, T. Cao, D. Liu, *Acc. Chem. Res.* **2017**, *50*, 659.
[49] W. Guo, C. H. Lu, R. Orbach, F. Wang, X. J. Qi, A. Cecconello, D. Seliktar, I. Willner, *Adv. Mater.* **2015**, *27*, 73.
[50] Y. Bi, X. Du, P. He, C. Wang, C. Liu, W. Guo, *Small* **2020**, *16*, 1906998.
[51] R. An, Y. Jia, B. Wan, Y. Zhang, P. Dong, J. Li, X. Liang, *PLoS One* **2014**, *9*, e115950.
[52] Y. Hu, S. Gao, H. Lu, J. Y. Ying, *J. Am. Chem. Soc.* **2022**, *144*, 5461.
[53] S. Chakraborty, S. Sharma, P. K. Maiti, Y. Krishnan, *Nucleic Acids Res.* **2009**, *37*, 2810.
[54] J. Choi, T. Majima, *Chem. Soc. Rev.* **2011**, *40*, 5893.
[55] Z. Huang, B. Liu, J. Liu, *Langmuir* **2016**, *32*, 11986.
[56] S. Saha, D. Bhatia, Y. Krishnan, *Small* **2010**, *6*, 1288.
[57] S. Saha, K. Chakraborty, Y. Krishnan, *Chem. Commun.* **2012**, *48*, 2513.
[58] G. Yao, J. Li, Q. Li, X. Chen, X. Liu, F. Wang, Z. Qu, Z. Ge, R. P. Narayanan, D. Williams, H. Pei, X. Zuo, L. Wang, H. Yan, B. L. Feringa, C. Fan, *Nat. Mater.* **2020**, *19*, 781.
[59] O. Suss, L. Motiei, D. Margulies, *Molecules* **2021**, *26*, 2828.
[60] J. Nygren, N. Svanvik, M. Kubista, *Biopolymers* **1998**, *46*, 39.
[61] F. Puoci, F. Iemma, R. Muzzalupo, U. G. Spizzirri, S. Trombino, R. Cassano, N. Picci, *Macromol. Biosci.* **2004**, *4*, 22.
[62] S. Tabassum, W. M. Al–Asbahy, M. Afzal, M. shamsi, F. Arjmand, *J. Lumin.* **2012**, *132*, 3058.
[63] Y. Hu, J. Y. Ying, *Mater. Today* **2022**, https://doi.org/10.1016/j.mattod.2022.12.003.

© 2023 Wiley-VCH GmbH

16136829, 2023, 12, Downloaded from https://onlinelibrary.wiley.com/doi/10.1002/smll.202205909 by Guangzhou University, Wiley Online Library on [20/02/2024]. See the Terms and Conditions (https://onlinelibrary.wiley.com/terms-and-conditions) on Wiley Online Library for rules of use; OA articles are governed by the applicable Creative Commons License